Supporting information

Geometric and Electronic Structure of the Mn(IV)Fe(III) Cofactor in Class Ic Ribonucleotide Reductase: Correlations to the Class Ia Binuclear Non-Heme Iron Enzymes

Yeonju Kwak[1], Wei Jiang[2,3], Laura M.K. Dassama[2], Kiyoung Park[1], Caleb B. Bell, III.[1], Lei V. Liu[1], Shaun D. Wong[1], Makina Saito[4], Yasuhiro Kobayashi[4], Shinji Kitao[4], Makoto Seto[4], Yoshitaka Yoda[5], E. Ercan Alp[6], Jiyong Zhao[6], J Martin Bollinger, Jr.*[,2,3], Carsten Krebs*[,2,3], and Edward I. Solomon*[,1]

[1]Department of Chemistry, Stanford University, Stanford, California 94305, United States
[2]Department of Biochemistry and Molecular Biology and [3]Chemistry, The Pennsylvania State University, University Park, Pennsylvania 16802, United States
[4]Research Reactor Institute, Kyoto University, Kumatori-Cho, Osaka 590-0494, Japan
[5]Spring 8/JASRI, 1-1-1 Kouto, Mikazuki-Cho, Sayo-gun, Hyogo 679-5198, Japan
[6]Advanced Photon Source, Argonne National Laboratory, Illinois 60439, United States

Figure S1. 4.2-K/0-mT Mössbauer spectrum of a sample containing the Mn^{IV}/Fe^{III} cofactor of *Ct* RNR-R2 (vertical bars).

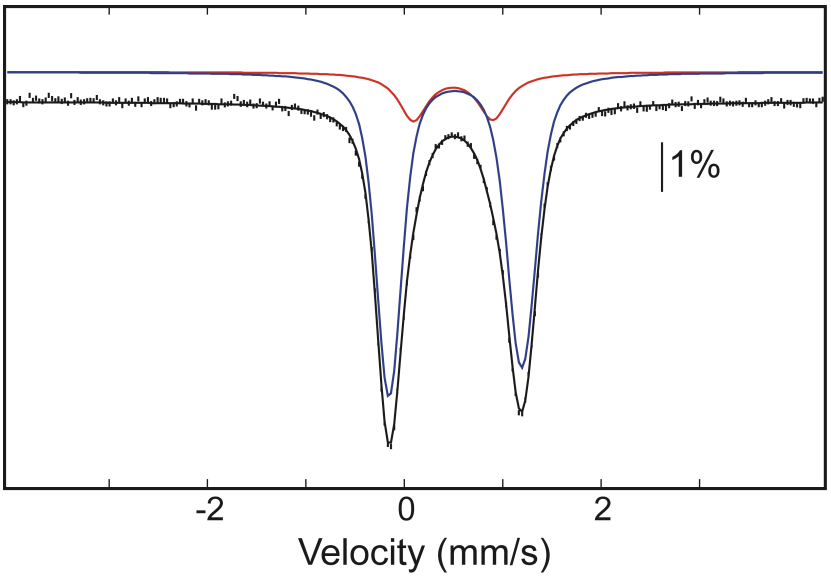

The sample was prepared as previously described (ref.22) to maximize the yield of the cofactor and minimize the formation of catalytically inactive $Fe_2^{III/III}$ clusters. The solid red and blue spectra are simulations of the $Fe_2^{III/III}$ and Mn^{IV}/Fe^{III} components, respectively, using parameters provided in Table S 2.1. The solid black line is the sum of the red and blue spectra. The ratio of Mn^{IV}/Fe^{III} to $Fe_2^{III/III}$ is ~6.5:1, a yield comparable to the best preparations of the Mn^{IV}/Fe^{III} cofactor *in vitro*.

Table S1. Mössbauer parameters used to simulate spectra in Figure S1.

Parameter	Mn^{IV}/Fe^{III}	$Fe_2^{III/III}$
δ (mm/s)	0.52	0.50
ΔE_Q (mm/s)	1.35	0.80
Rel. Area (%)	85	15

Figure S2. 4.2-K/53-mT Mössbauer spectrum of the Mn/Fe-*Ct* RNR-R2 used in this study.

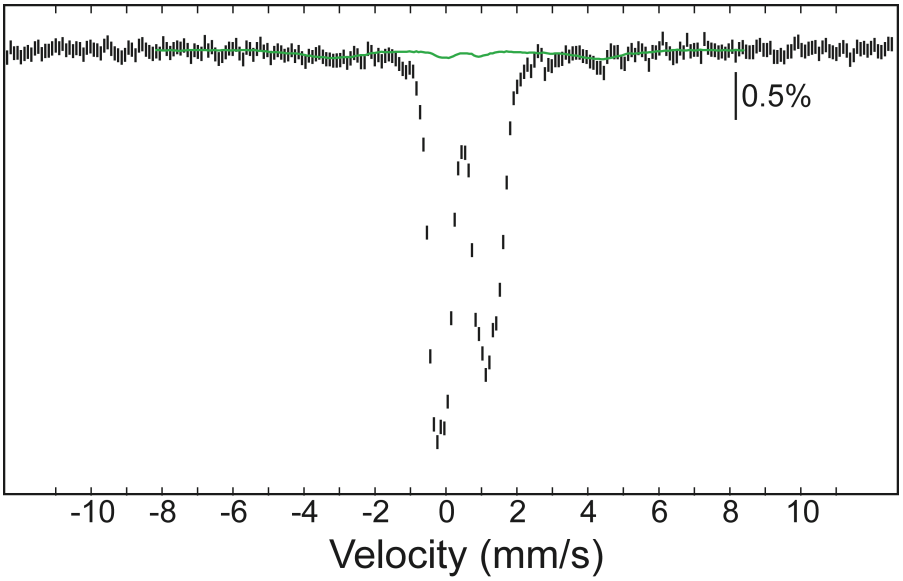

The spectrum (black vertical bars), acquired over a wider range of Doppler velocities reveals a minor contribution from the Mn^{III}/Fe^{III} cluster. This S=1/2 cluster exhibits a broad, magnetically split spectrum (see absorption intensities at ~ +4 and -4 mm/s) with the addition of a small externally applied magnetic field. Based on the experimental "reference" spectrum (solid green line) of a sample prepared to contain only the Mn^{III}/Fe^{III} cluster, the contribution of this component to the spectrum is estimated to be 7-10%.

Figure S3. Simulated NRVS spectra for different structures of $Mn^{IV}Fe^{III}$ intermediate. Core structures are shown as an inset for each spectrum.

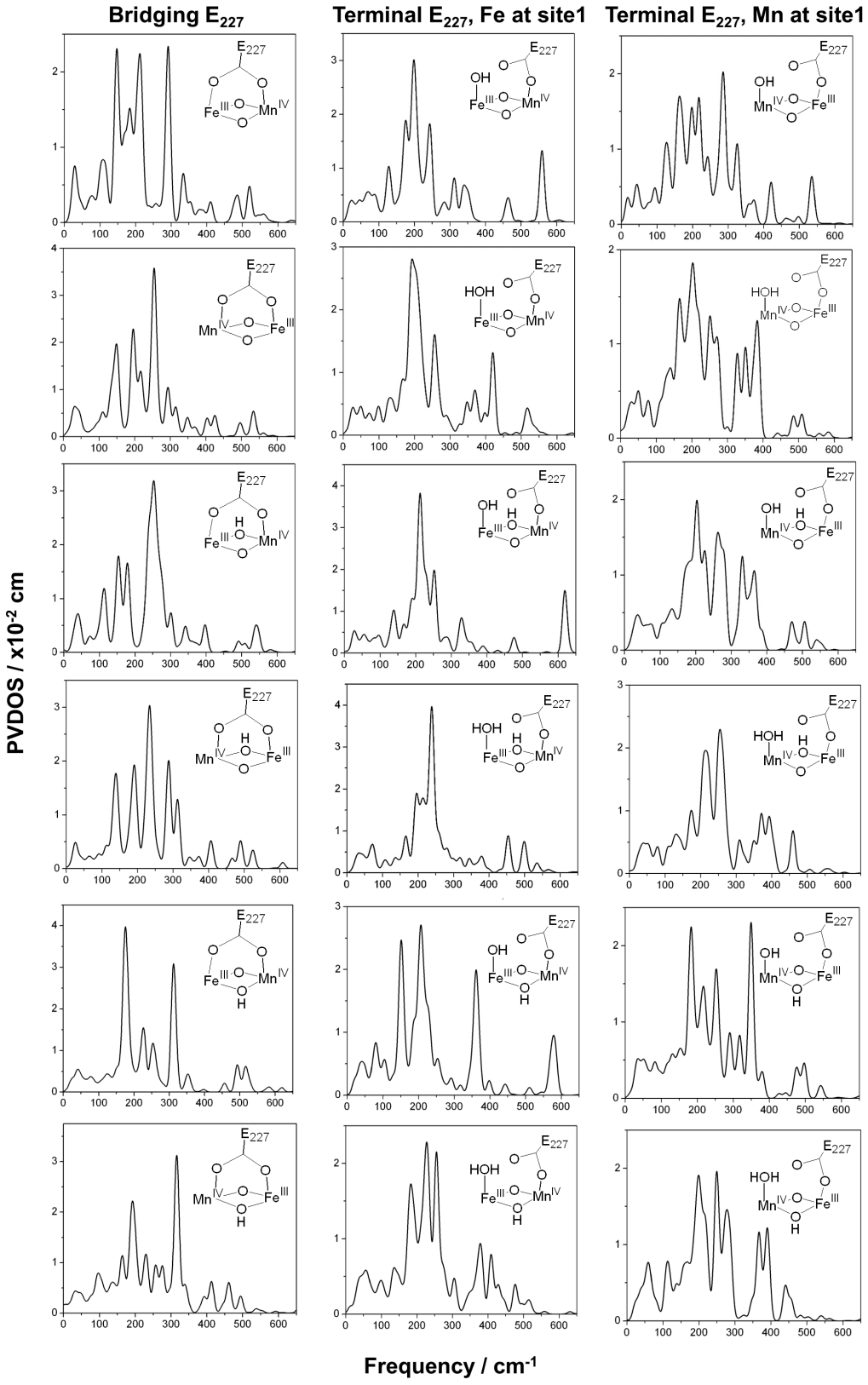

Figure S4. MCD spectra on $Mn^{IV}Fe^{III}$ intermediate with different temperatures and fields

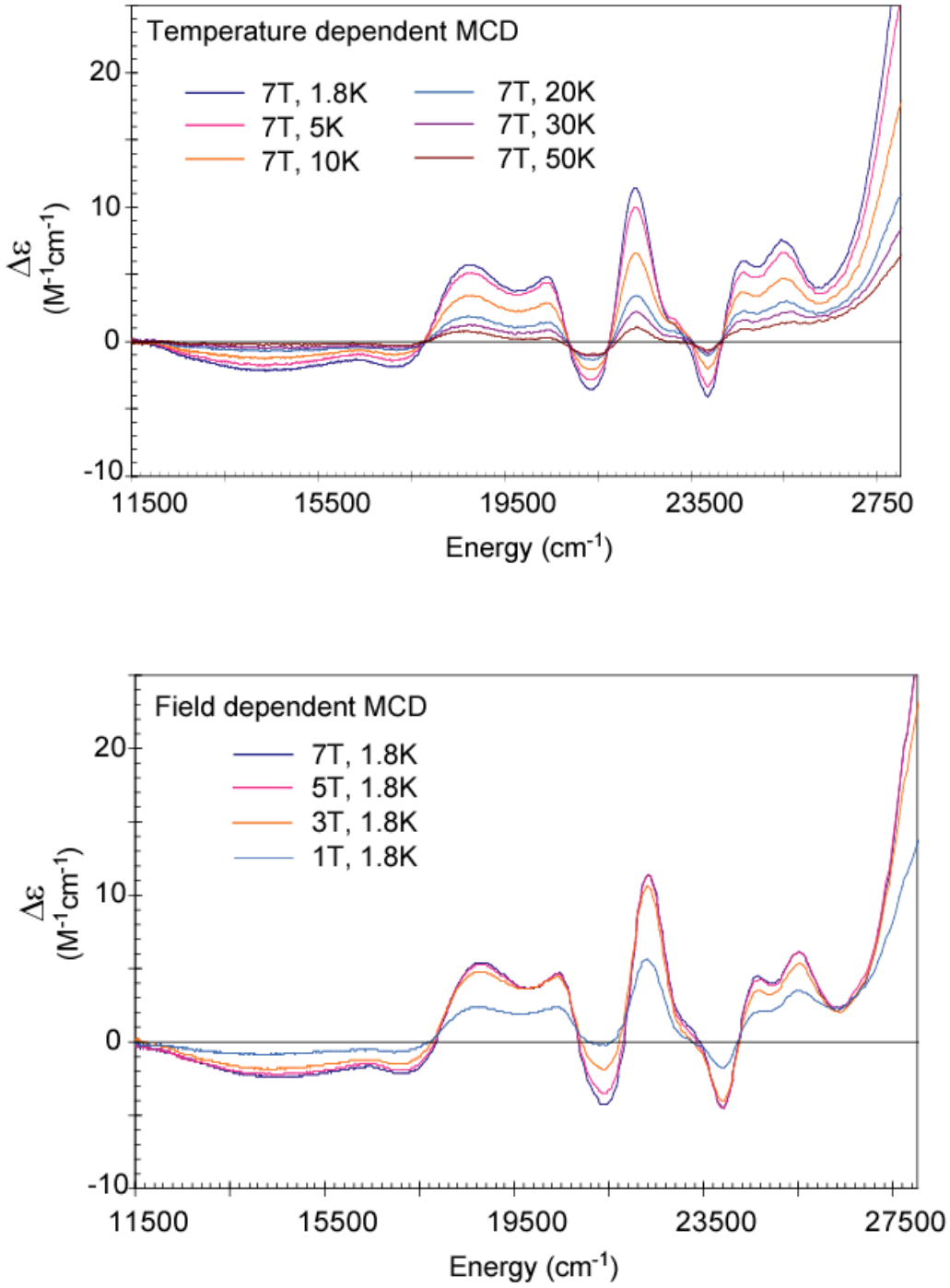

Figure S5. Room temperature /Low temperature absorption (upper) and CD (lower) spectra of the $Mn^{IV}Fe^{III}$ intermediate

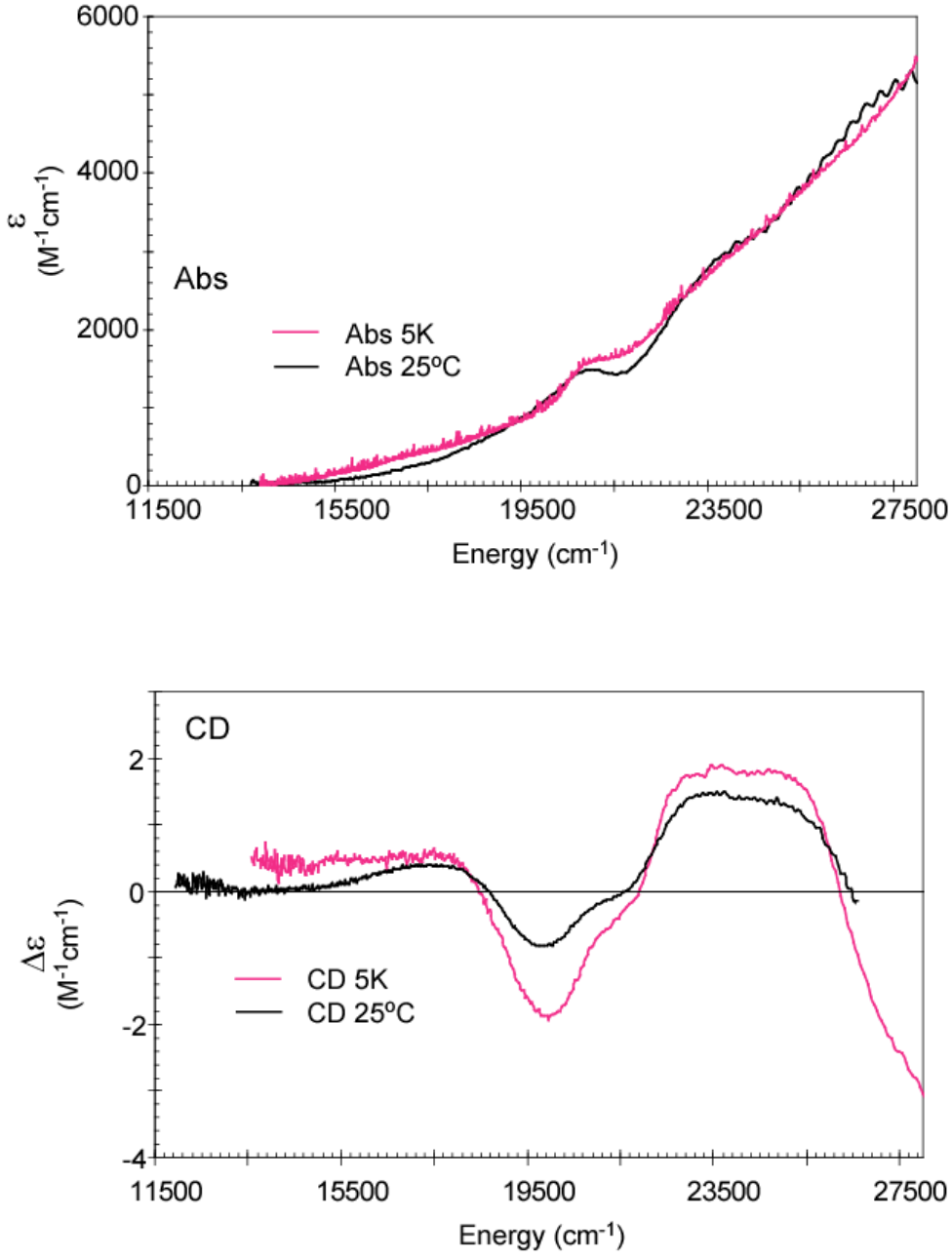

Figure S6. MCD spectra of $Fe^{III}Fe^{III}$ *Ct* RNR control

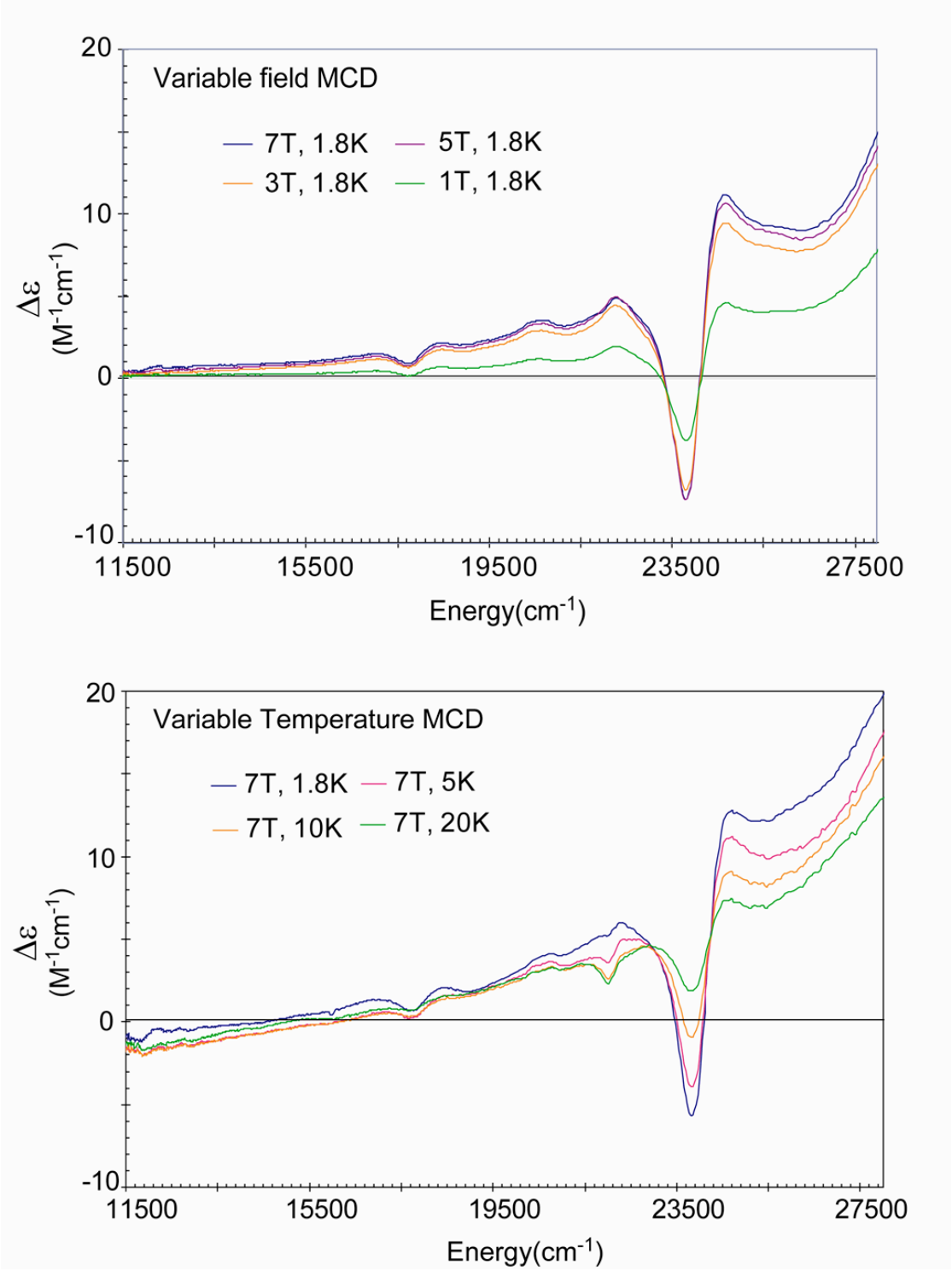

Figure S7. (a) crystal and computational structure of $[Mn^{IV}(\mu\text{-}O)_2Mn^{III}(OAc)(Tpen)]^{3+}$ model complex (MnTpen) used; (b) ligand to metal CT to Mn^{IV} site comparison between experimental observation and TD DFT calculation; and (c) spectroscopic and experimental d-d transitions for Mn^{III} and Mn^{IV}. (Adapted and modified from reference 53)

(a)

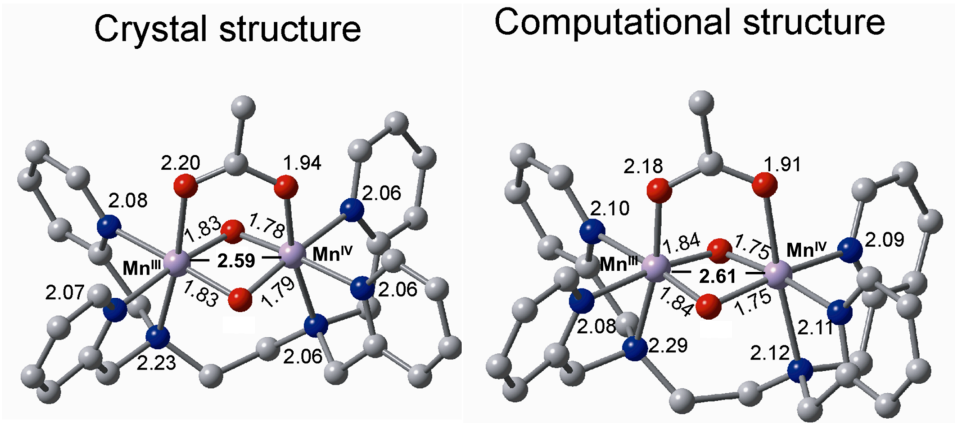

(b)

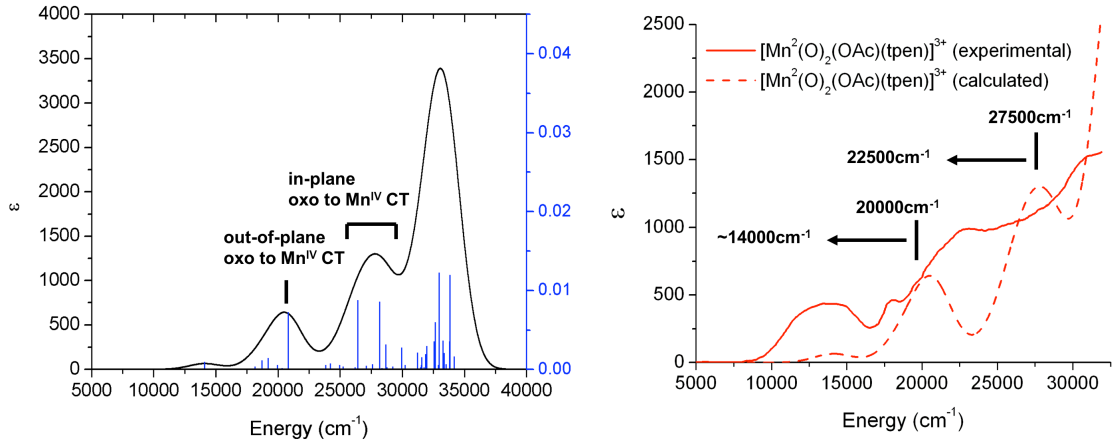

(c)

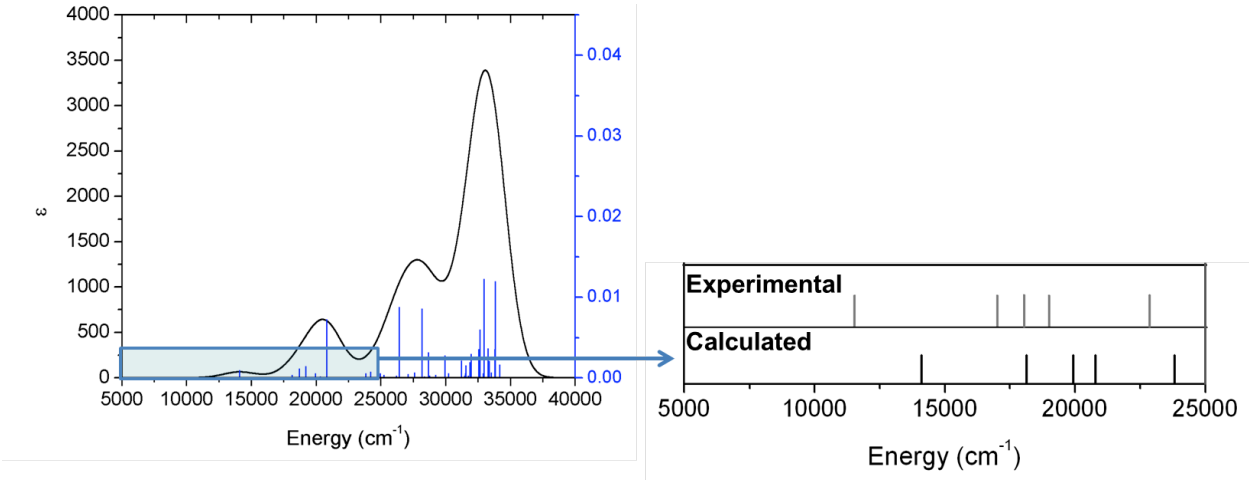

Figure S8-1. Structure of (a) bis-μ-oxo $Fe^{III}Fe^{III}$ model complex ($[Fe_2(\mu\text{-}O)_2(6TLA)_2]^{2-}$); and (b) μ-oxo, μ-hydroxo $Fe^{III}Fe^{III}$ model complex ($[Fe_2(\mu\text{-}O)(\mu\text{-}OH)(6TLA)_2]^{2-}$). Adapted from ref 54-56

(a)

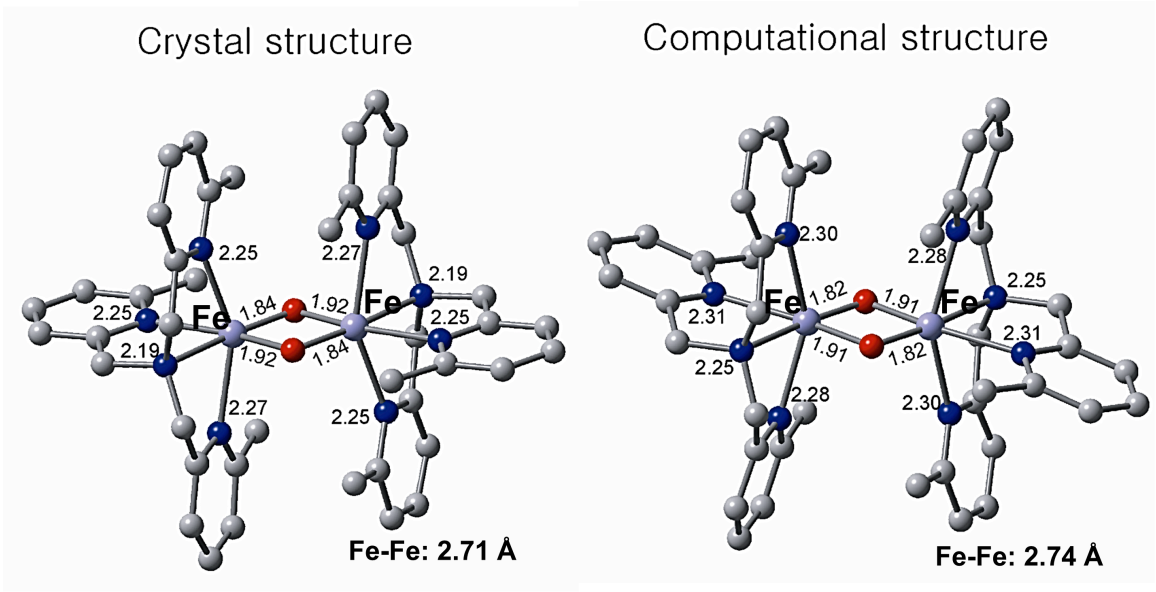

(b)

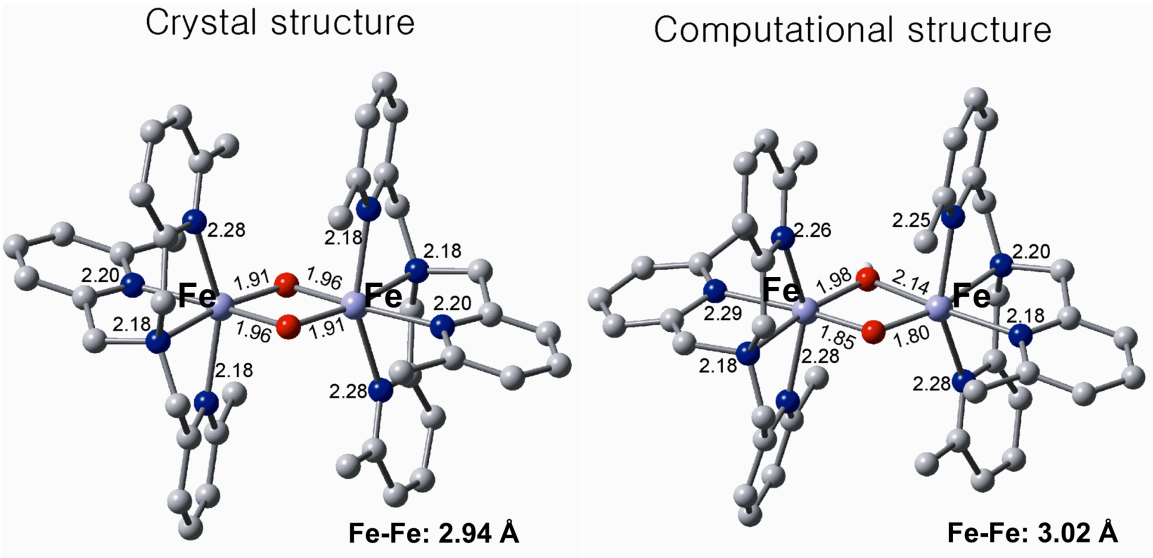

Figure S8-2. (a) experimental Abs data on Fe^{III}-(μ-O)$_2$-Fe^{III} & Fe^{III}-(μ-O, μ-OH)-Fe^{III} model complex (from S8-1); (b) TD DFT of Fe^{III}-(μ-O)$_2$-Fe^{III} & Fe^{III}-(μ-O, μ-OH)-Fe^{III} model complex; (c) comparison between experimental Abs and calculated TD DFT energy. Adapted and modified from reference 56.

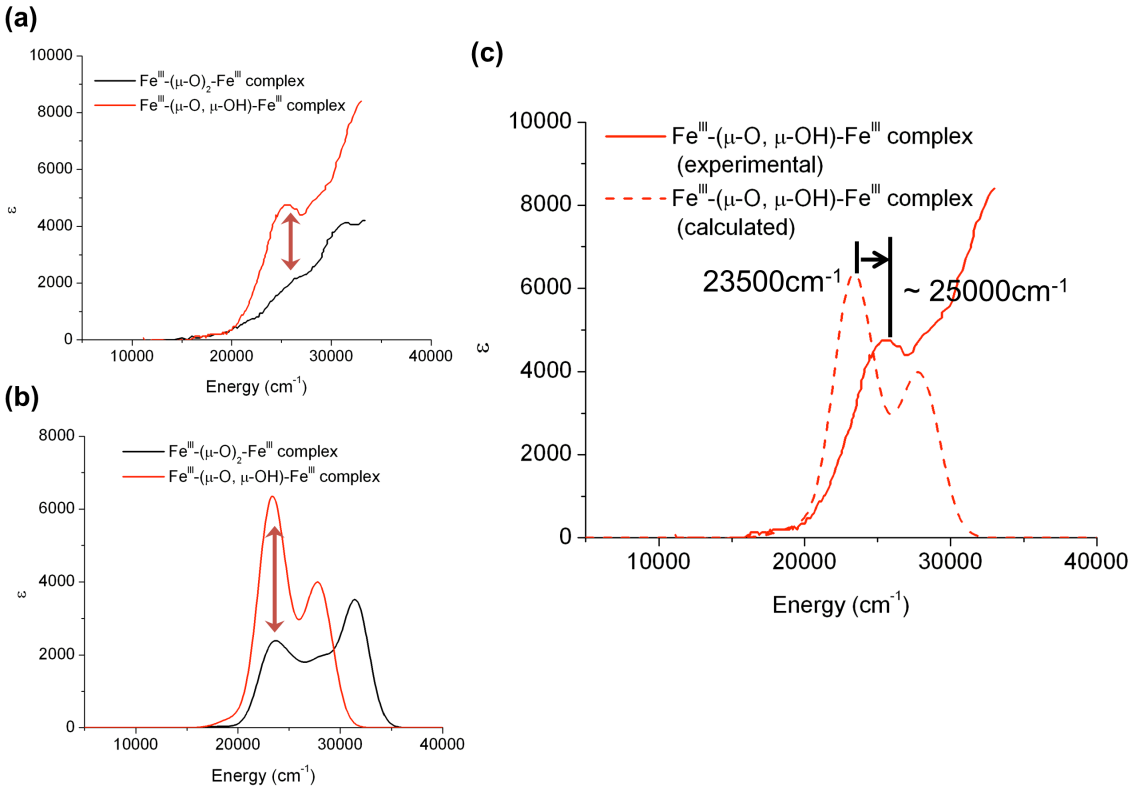

Figure S9. Gaussian broadened TD DFT calculation for μ-oxo to Fe^{III} CT transitions (first 40 transitions) of (a) GaFe structure with terminal OH on Ga^{III}, (b) GaFe structure with terminal water on Ga^{III}. Both have μ-oxo, μ-hydroxo bridges.

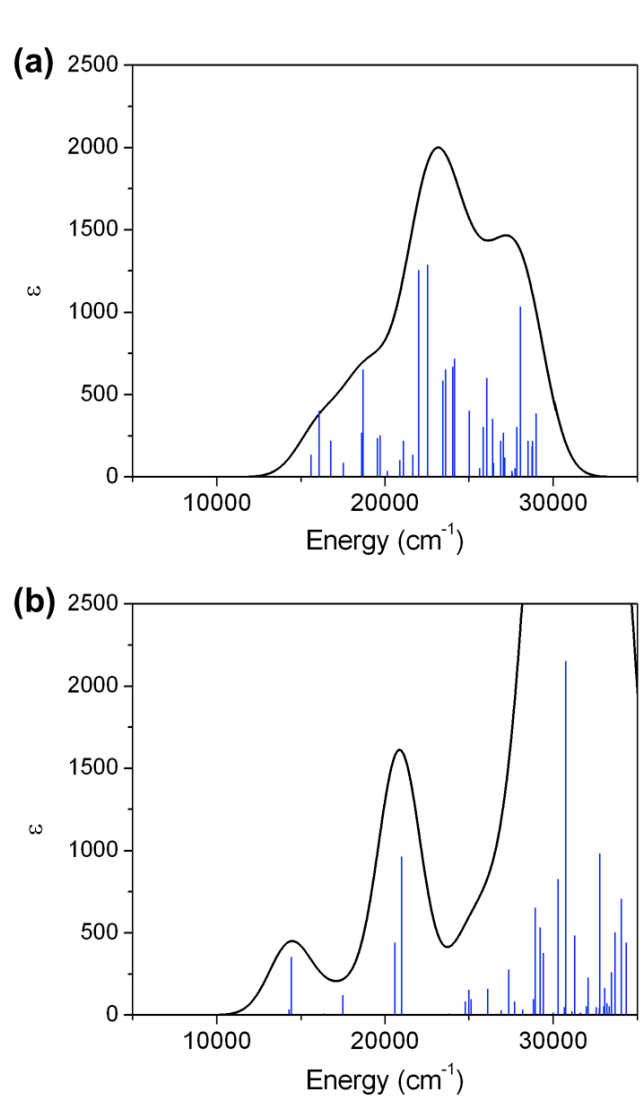

S10. Structure used for $Mn^{IV}Fe^{III}$ TD DFT computation

(a) $Mn^{IV}Ga^{III}$ active site with terminal OH on Mn^{IV}, μ-O, μ -OH bridges

C	5.31358800	-2.04215900	-2.16784900
C	4.55443500	-2.91404800	-1.15479900
C	3.89034900	-2.03094500	-0.08329900
O	2.89661600	-1.34280500	-0.56438700
O	4.37412300	-1.96664100	1.04699500
C	2.62946400	1.48694900	-4.15691400
C	1.23977500	1.86282800	-3.62323700
C	0.79435700	1.08721300	-2.37208700
O	1.70602100	0.75383300	-1.55705500
O	-0.44753200	0.86644200	-2.26018500
C	5.01161400	1.06778900	0.49334800
C	3.89663000	1.49153900	1.39547100
N	2.58231300	1.05008300	1.29275400
C	3.98191900	2.33075400	2.47720200
C	1.90612500	1.59252700	2.29086300
N	2.71296900	2.38146500	3.03307400
C	-4.42647400	-3.64908400	-0.23950900
C	-3.25813600	-3.04265900	-1.03142500
C	-3.59261600	-1.67059400	-1.64071500
O	-4.74407200	-1.43616500	-2.00808600
O	-2.59964300	-0.82969900	-1.83065500
C	-2.95650900	-0.30263000	3.94052800
C	-3.29304800	-1.49462700	3.03672300
C	-2.26738700	-1.53627000	1.90312200
O	-1.28300200	-2.27758400	2.01007300
O	-2.53021100	-0.70865200	0.94324000
C	-5.05239200	1.41178800	-0.43641500
C	-3.83771400	2.28999600	-0.40341400
N	-2.52325900	1.82899300	-0.41185300
C	-3.80926500	3.65955600	-0.31655100
C	-1.73910200	2.88639200	-0.32155800
N	-2.47238100	4.02297600	-0.26346500
H	4.62582100	-1.33680600	-2.64483600
H	6.10159300	-1.46383200	-1.66950700
H	5.78804600	-2.64961900	-2.94982600
H	5.23803600	-3.60950400	-0.65633800
H	3.78407500	-3.49427900	-1.67708700
H	2.90009700	2.11315400	-5.01610200
H	3.38597100	1.60940500	-3.37712800
H	2.65659300	0.43963000	-4.47861400
H	1.22645000	2.93020100	-3.35464800
H	0.46785600	1.72857600	-4.38771400
H	5.28903800	0.03372900	0.71883700
H	4.69689700	1.10699900	-0.55437600
H	5.87901300	1.72262200	0.63203500
H	4.81729100	2.87301800	2.89274100
H	0.85331000	1.42243900	2.45691500
H	2.43797300	2.88464900	3.86208900
H	-5.32815900	-3.68032100	-0.85837800
H	-4.18708600	-4.66437100	0.09985100
H	-4.65080800	-3.04061400	0.64350500

H	-3.01017700	-3.70024000	-1.87936500
H	-2.35524100	-2.98079500	-0.41988800
H	-3.65128500	-0.22504000	4.78727100
H	-3.00325500	0.63057100	3.36931100
H	-1.94152600	-0.40460100	4.34190500
H	-4.30375800	-1.38236700	2.62860200
H	-3.23722700	-2.43122000	3.60056000
H	-5.95783200	2.02711500	-0.47731900
H	-5.03243700	0.72322400	-1.28879600
H	-5.08971200	0.78502900	0.46185500
H	-4.60556300	4.38753100	-0.28376000
H	-0.66254100	2.83150900	-0.26351100
H	-2.10476900	4.95979700	-0.20521700
O	-0.02534000	0.68859000	0.54057000
O	1.29727800	-1.31761400	1.66834100
H	0.38103300	-1.68062800	1.73148800
O	0.13442200	-1.45539300	-0.72018800
H	0.45451900	-1.62822500	-1.61945000
Mn	1.39500600	-0.33395500	0.19987300
Ga	-1.38054800	-0.08476900	-0.55128700

(b) $Ga^{III}Fe^{III}$ active site with terminal OH on Ga^{III}, μ -O, μ -OH bridges

C	5.31358400	-2.04215900	-2.16784600
C	4.58079300	-2.94650500	-1.14094900
C	3.97375200	-2.06375100	-0.02838500
O	2.95652500	-1.31646800	-0.48662500
O	4.50590500	-2.01136700	1.12620600
C	2.62946600	1.48694800	-4.15691600
C	1.41952900	2.13252500	-3.43099600
C	0.90882100	1.30599500	-2.22875300
O	1.81768100	0.90873700	-1.37113400
O	-0.37494000	1.08793000	-2.15700500
C	5.01161500	1.06779100	0.49334700
C	3.94823100	1.44013900	1.48675900
N	2.61385300	0.97447300	1.44761200
C	4.08621300	2.24332000	2.62274900
C	1.97157800	1.46623700	2.52599600
N	2.83353700	2.24391400	3.26862700
C	-4.42647400	-3.64908400	-0.23950900
C	-3.31464200	-3.10758300	-1.17562200
C	-3.64163500	-1.70040500	-1.72827300
O	-4.82997600	-1.40614200	-2.09623500
O	-2.61201300	-0.84097200	-1.83011100
C	-2.95651000	-0.30263200	3.94052400
C	-3.20575700	-1.59255000	3.11784000
C	-2.14361500	-1.62939400	2.00921900
O	-1.04872200	-2.26830600	2.22684300
O	-2.44015500	-0.90972000	0.94067700
C	-5.05239200	1.41178800	-0.43641100
C	-3.86166800	2.31716200	-0.27416300
N	-2.51452700	1.87040000	-0.24483900
C	-3.86021400	3.70417300	-0.09039000
C	-1.73492400	2.95086000	-0.04111000
N	-2.51155400	4.08980800	0.05539300
H	4.59955700	-1.32270900	-2.60545800
H	6.12598600	-1.47291900	-1.67658900

H	5.76145800	-2.64127300	-2.98543000
H	5.28056200	-3.66509900	-0.67677100
H	3.77188200	-3.50557800	-1.64833900
H	3.00734500	2.14980600	-4.95947700
H	3.44171800	1.29452400	-3.43470700
H	2.34301300	0.52050500	-4.61169500
H	1.71764600	3.12875400	-3.04192800
H	0.56843300	2.27843600	-4.11929300
H	5.36394300	0.04259800	0.70688000
H	4.59907500	1.07615600	-0.53026200
H	5.86210400	1.77108400	0.55639000
H	4.95054500	2.77189300	3.01474000
H	0.92836400	1.26420200	2.74973400
H	2.60173200	2.71523200	4.14053800
H	-5.40567100	-3.60417900	-0.74957200
H	-4.21692800	-4.69480500	0.05868600
H	-4.48608100	-3.03125800	0.67408400
H	-3.20612200	-3.78171900	-2.05233800
H	-2.33974600	-3.07055800	-0.66081300
H	-3.69465400	-0.19628300	4.76003700
H	-3.02987700	0.58325000	3.28404600
H	-1.94462500	-0.32335300	4.38616300
H	-4.21604000	-1.57031700	2.67089500
H	-3.10028500	-2.48888800	3.75459200
H	-5.97996700	2.00563000	-0.52367300
H	-4.94933100	0.75423800	-1.32094100
H	-5.14045300	0.73388900	0.43330100
H	-4.68033200	4.41621400	-0.05272900
H	-0.65264800	2.90752200	0.05255000
H	-2.16537400	5.03731200	0.19444600
O	0.00649000	0.65332500	0.65135000
O	1.36458400	-1.40836900	1.70866500
H	0.41556700	-1.79989900	1.81914600
O	0.20986300	-1.33588200	-0.73450100
H	0.61916600	-1.81307200	-1.49665600
Ga	1.47854000	-0.31284500	0.30360400
Fe	-1.37175800	-0.00328000	-0.53632500

(c) $Mn^{IV}Ga^{III}$ active site with terminal H_2O on Mn^{IV}, μ -O, μ -OH bridges

C	5.47031400	-2.08425600	-1.75503600
C	4.58487300	-2.90779000	-0.80969400
C	3.61267100	-2.13500600	0.08676600
O	3.09577000	-1.05460400	-0.41197400
O	3.34262200	-2.60104100	1.21008500
C	2.73487200	1.16519200	-4.11592900
C	1.31283900	1.59941500	-3.73850200
C	0.82251800	1.03187000	-2.41157500
O	1.74453200	0.85010600	-1.52849100
O	-0.39569000	0.78931100	-2.26363900
C	5.05711900	1.26408500	0.58223500
C	3.91289600	1.86726200	1.32542600
N	2.58231200	1.48440200	1.17971900
C	3.97134800	2.85661300	2.27195400
C	1.87039000	2.21792100	2.02689800
N	2.67387400	3.06122800	2.70322600
C	-4.25734500	-3.73184000	0.20147600

C	-3.07810300	-3.16973700	-0.60748000
C	-3.42043300	-1.87312900	-1.35082700
O	-4.56387300	-1.65854700	-1.72889700
O	-2.40947600	-1.05823000	-1.63998800
C	-2.92717000	0.04465400	4.04869200
C	-3.03481500	-1.27705300	3.27524000
C	-1.98819100	-1.26087800	2.17289800
O	-0.89820900	-1.82568200	2.37112500
O	-2.33523300	-0.58014600	1.13100500
C	-4.99737600	1.26823800	-0.50177600
C	-3.82404700	2.19381900	-0.57929000
N	-2.48168800	1.80822100	-0.53589300
C	-3.86607300	3.56097800	-0.67430400
C	-1.75747700	2.91597700	-0.59545600
N	-2.55405300	4.00042600	-0.68164900
H	4.86213700	-1.44728200	-2.40409500
H	6.15552000	-1.43614200	-1.19638700
H	6.07453700	-2.74706000	-2.38381800
H	5.18710300	-3.54152400	-0.15146900
H	3.96036500	-3.59252800	-1.40253000
H	3.02015100	1.59902000	-5.08049600
H	3.45675200	1.48663500	-3.36129900
H	2.80490600	0.07557300	-4.20165800
H	1.26467300	2.69507400	-3.65641800
H	0.58367800	1.31443000	-4.50278400
H	5.27569300	0.25454300	0.94656400
H	4.83571700	1.17885100	-0.48519200
H	5.95353300	1.87759400	0.71287400
H	4.80723600	3.41444700	2.66430600
H	0.80169500	2.13353300	2.14451300
H	2.37314900	3.71234500	3.41345700
H	-5.13201000	-3.86159300	-0.44148100
H	-3.99744000	-4.69766400	0.64932400
H	-4.53895200	-3.04662800	1.00851600
H	-2.77961200	-3.89584600	-1.37883100
H	-2.19571700	-3.01985000	0.02039300
H	-3.65354900	0.08404700	4.86858900
H	-3.11378400	0.89486000	3.38441100
H	-1.92571200	0.15772700	4.47967600
H	-4.03459400	-1.37767200	2.84116200
H	-2.84272300	-2.12680200	3.93604700
H	-5.92497300	1.84033600	-0.59928200
H	-4.95967400	0.49593500	-1.27756700
H	-5.00932600	0.74325100	0.46025100
H	-4.70196300	4.24036300	-0.73340900
H	-0.68069500	2.94470600	-0.55808300
H	-2.24223900	4.95714400	-0.75518500
O	0.04687200	0.87195300	0.52420900
O	1.46964100	-0.95007000	1.85869500
H	0.53626700	-1.33444500	1.99575500
H	2.14803900	-1.70449100	1.77023300
O	0.33045500	-1.30428400	-0.54601100
H	0.60089400	-1.64914700	-1.41224700
Mn	1.49761000	-0.00753000	0.16452100
Ga	-1.36181200	-0.02743800	-0.47108200

(d) $Ga^{III}Fe^{III}$ active site with terminal H_2O on Ga^{III}, μ -O, μ -OH bridges

C	5.47031200	-2.08425600	-1.75503400
C	4.76764300	-2.95120200	-0.68610800
C	3.74820700	-2.21300200	0.18882700
O	3.15672900	-1.14142300	-0.33519000
O	3.47597500	-2.67303500	1.36896800
C	2.73487400	1.16519100	-4.11593000
C	1.50307000	1.89379700	-3.51171300
C	0.96157600	1.21511800	-2.24707200
O	1.87614100	0.94204400	-1.32283700
O	-0.30157400	0.95879400	-2.14737500
C	5.05711700	1.26408700	0.58223400
C	3.96481800	1.72394100	1.49996600
N	2.62153800	1.28745100	1.42498800
C	4.06554700	2.61078100	2.57401000
C	1.93747700	1.88347600	2.42830300
N	2.78393700	2.69413700	3.14600700
C	-4.25734600	-3.73184100	0.20147600
C	-3.14853600	-3.27356700	-0.78401000
C	-3.48630700	-1.93414700	-1.46300100
O	-4.64983300	-1.66723600	-1.88699000
O	-2.45390900	-1.05418700	-1.61312400
C	-2.92717000	0.04465200	4.04868900
C	-3.00497500	-1.33861700	3.35027900
C	-1.89873300	-1.36976100	2.29922700
O	-0.73632400	-1.80310600	2.65305200
O	-2.21559000	-0.86777900	1.12150400
C	-4.99737300	1.26823900	-0.50177300
C	-3.83161500	2.21228900	-0.40063800
N	-2.46600500	1.82109200	-0.32215300
C	-3.87957200	3.60720200	-0.33460900
C	-1.72979100	2.94941200	-0.20518500
N	-2.55119800	4.05469800	-0.21218000
H	4.72601000	-1.57179700	-2.38766800
H	6.10439400	-1.30943100	-1.28628600
H	6.11485500	-2.71182400	-2.39790100
H	5.49216300	-3.43480200	-0.00623800
H	4.21060600	-3.77567600	-1.17892600
H	3.12296200	1.72864000	-4.98408100
H	3.53480400	1.07159600	-3.36237600
H	2.46312800	0.15046300	-4.45944700
H	1.79129100	2.92838200	-3.23478300
H	0.67426200	1.95593700	-4.23740400
H	5.42143700	0.26197000	0.87342700
H	4.68622600	1.18534800	-0.45309900
H	5.90907800	1.96507900	0.61478800
H	4.91988100	3.15880000	2.96018400
H	0.88140700	1.72490300	2.62265900
H	2.52192700	3.24793100	3.96026400
H	-5.23591400	-3.75689500	-0.30878300
H	-4.03223600	-4.74021200	0.59559900
H	-4.33098200	-3.03287500	1.05328100
H	-3.04023700	-4.02506900	-1.59382300
H	-2.17150900	-3.18505500	-0.28000500
H	-3.71316900	0.13851500	4.82090300
H	-3.06488700	0.85793900	3.31349300
H	-1.94566300	0.17424500	4.54018400
H	-3.98810800	-1.46833800	2.86649800

H	-2.83891500	-2.15070900	4.07845100
H	-5.93669700	1.83469800	-0.62222800
H	-4.88827200	0.56588300	-1.34859400
H	-5.07681100	0.64548200	0.40888100
H	-4.72651800	4.28658200	-0.36541800
H	-0.64863900	2.97126500	-0.10662700
H	-2.24616700	5.02511500	-0.15274900
O	0.08779800	0.75605900	0.69243700
O	1.52690800	-1.16108400	1.89427400
H	0.54363900	-1.48224500	2.16373800
H	2.29449800	-1.88150900	1.86124100
O	0.37811600	-1.28081900	-0.58459400
H	0.73668000	-1.76840900	-1.36703300
Ga	1.57405900	-0.08389600	0.31419700
Fe	-1.33267866	-0.02029254	-0.46333934

Full reference on Gaussian 09 Software package

Gaussian 09, Revision D.01, Frisch, M. J.; Trucks, G. W.; Schlegel, H. B.; Scuseria, G. E.; Robb, M. A.; Cheeseman, J. R.; Scalmani, G.; Barone, V.; Mennucci, B.; Petersson, G. A.; Nakatsuji, H.; Caricato, M.; Li, X.; Hratchian, H. P.; Izmaylov, A. F.; Bloino, J.; Zheng, G.; Sonnenberg, J. L.; Hada, M.; Ehara, M.; Toyota, K.; Fukuda, R.; Hasegawa, J.; Ishida, M.; Nakajima, T.; Honda, Y.; Kitao, O.; Nakai, H.; Vreven, T.; Montgomery, Jr., J. A.; Peralta, J. E.; Ogliaro, F.; Bearpark, M.; Heyd, J. J.; Brothers, E.; Kudin, K. N.; Staroverov, V. N.; Kobayashi, R.; Normand, J.; Raghavachari, K.; Rendell, A.; Burant, J. C.; Iyengar, S. S.; Tomasi, J.; Cossi, M.; Rega, N.; Millam, J. M.; Klene, M.; Knox, J. E.; Cross, J. B.; Bakken, V.; Adamo, C.; Jaramillo, J.; Gomperts, R.; Stratmann, R. E.; Yazyev, O.; Austin, A. J.; Cammi, R.; Pomelli, C.; Ochterski, J. W.; Martin, R. L.; Morokuma, K.; Zakrzewski, V. G.; Voth, G. A.; Salvador, P.; Dannenberg, J. J.; Dapprich, S.; Daniels, A. D.; Farkas, Ö.; Foresman, J. B.; Ortiz, J. V.; Cioslowski, J.; Fox, D. J. Gaussian, Inc., Wallingford CT, 2009.